



Published in final edited form as:

Sci Signal. ; 3(130): ra52. doi:10.1126/scisignal.2000762.

Regulation of Notch1 Signaling by Nrf2: Implications for Tissue Regeneration

Nobunao Wakabayashi^{1,*}, Soona Shin³, Stephen L. Slocum², Elin S. Agoston^{3,†}, Junko Wakabayashi^{1,‡}, Mi-Young Kwak⁵, Vikas Misra^{1,#}, Shyam Biswal¹, Masayuki Yamamoto⁶, and Thomas W. Kensler^{1,2,3}

¹ Department of Environmental Health Sciences, The Johns Hopkins University, Baltimore, MD 21205, US

² Department of Biochemistry and Molecular Biology, Bloomberg School of Public Health, The Johns Hopkins University, Baltimore, MD 21205, US

³ Department of Pharmacology and Molecular Sciences, School of Medicine, The Johns Hopkins University, Baltimore, MD 21205, US

⁵ College of Pharmacy, Yeungnam University, 214-1 Dae-dong, Gyeongsan-si, Gyeongsangbuk-do, 712-749, South Korea

⁶ Department of Medical Biochemistry, Tohoku University Graduate School of Medicine, 2-1 Seiryochō, Aoba-ku, Sendai 980-8575, Japan

Abstract

The Keap1-Nrf2-ARE signaling pathway evokes an adaptive response for cell survival following endogenous (for example, inflammation) and exogenous (for example, carcinogens) stresses. Keap1 inhibits the transcriptional activation activity of Nrf2 in unstressed cells by facilitating its degradation. Through transcriptional analyses in *Keap1*- or *Nrf2*-disrupted mice, we identified interactions with the Notch1 signaling pathway. We found a functional antioxidant response element (ARE) recognized by Nrf2 in the promoter of *Notch1*. Notch1 regulates processes such as proliferation and cell fate decisions. We report a functional role for this cross talk between the two pathways and show that disruption of *Nrf2* impeded liver regeneration following partial hepatectomy and was rescued by re-establishment of Notch1 signaling.

Introduction

Nrf2 (p45 nuclear factor erythroid-derived 2-related factor 2) is a prosurvival transcription factor that plays a pivotal role in maintaining cellular homeostasis following electrophile and

*To whom correspondence should be addressed. Department of Pharmacology & Chemical Biology, BSTWR E1316, University of Pittsburgh, Pittsburgh, PA 15261, nw99@pitt.edu.

†present address: Brigham and Women's Hospital, Department of Pathology, Division of Women's & Perinatal Pathology, Boston, MA 02115

‡present address: Department of Cell Biology, Johns Hopkins University School of Medicine, Baltimore, MD 21205

#present address: Department of Cancer Immunology & AIDS, Dana-Farber Cancer Institute, Boston, MA 02115

Competing interests: *There may be MTAs related to the new mouse constructs, per the policy of Johns Hopkins University.*

Author contributions: NW designed and performed the research, established the NICD and compound genetically engineered mice, analyzed the data and wrote the manuscript; SS conducted the ChIP assays and together with JW conducted the RT-PCR analyses; SLS established the conditional Keap1 disrupted MEFs; ESA performed the RT-PCR in MEF and assisted in writing the manuscript; MK, VM and SB conducted and analyzed the initial microarray studies; MY provided the Nrf2 and Keap1 null mice and helped evaluate the data; and TWK helped initiate the project and assisted with research design and manuscript preparation.

oxidative stresses (1). Coordinated changes in response to Nrf2 activation result in enhanced expression of genes that contribute to (i) free radical metabolism, (ii) electrophile detoxication, (iii) glutathione biosynthesis, (iv) generation of reducing equivalents, (v) formation of direct antioxidants, (vi) toxin efflux transporters, (vii) the proteasomal system, as well as (viii) modulation of inflammatory pathways. Many of these genes contain *cis*-elements in their regulatory domains known as antioxidant response elements (AREs) (2). The ARE interacts with the cap 'n' collar (Cnc) family of basic leucine zipper (bZip) transcription factors, including Nrf2, and their dimerization partners that include other bZip transcription factors, such as the small Mafs (1). Experiments with knockout mice for various Cnc genes revealed that these transcription factors contribute to both constitutive and inducible expression of these cytoprotective genes (3).

Analysis of *Nrf2*-null mice revealed that Nrf2 is the primary factor in regulation of gene expression through the ARE *in vivo*. The knockout mice survive and produce viable offspring, but they are more sensitive towards toxicities associated with various electrophiles and reactive oxygen species than are wild-type mice (3,4). In early development, *Nrf2*-null mice appear normal. However, it has not been determined whether development in the knockout mice is altered under stressed conditions. By contrast, mice null for *Nrf1* (encoding a related Cnc bZip transcription factor) show a drastic phenotype in early development and are embryonic-lethal at mid-to-late gestation due to anemia caused by a non-cell autonomous defect in erythropoiesis in the fetal liver (5). This observation suggests a fundamental role for Nrf1 in development. Analysis of the liver-specific *Nrf1*-conditional knockout mouse indicates that Nrf1 contributes to postnatal ARE-dependent gene regulation as well as having a prenatal role (6). Because the *Nrf1::Nrf2* double knockout mouse has a shorter life span *in utero* than the *Nrf1* single knockout, Nrf2 has been proposed to contribute or partially compensate as a transcription factor in early development (7). Nrf2 influences tissue injury and repair. The increased abundance of Nrf2 in hepatocyte-specific *Keap1*-disrupted mice results in resistance to chemical- and inflammation-mediated hepatotoxicity (8,9). By contrast, *Nrf2*-null mice, which are more sensitive to hepatotoxins (10), exhibit significantly delayed liver regeneration following partial hepatectomy (11).

Differential microarray analyses have been conducted in several tissues of wild-type and *Nrf2*-null mice (12,13) to help define cytoprotective pathways and to characterize the role of the Keap1-Nrf2-ARE pathway in the pharmacodynamic action of several classes of anticarcinogens (14,15). However, these analyses reflect expression patterns from heterogeneous cell populations within the analyzed tissues. To overcome this limitation, immortalized mouse embryonic fibroblasts (MEFs) were established from *Keap1*^{-/-}, *Nrf2*^{-/-}, *Keap1*^{-/-}::*Nrf2*^{-/-}, and wild-type mice (16). These MEFs showed striking differential sensitivity to redox cycling quinones (17) and photooxidative damage from combined exposure to retinaldehyde and UVA light (18). Strong differential expression of *Notch1* and some of its downstream effectors was observed, raising the interesting possibility that the Notch1 signaling cascade may be regulated at the transcriptional level through interactions of Nrf2 with ARE. Levels of *Notch1* mRNA were substantially reduced in *Nrf2*-null MEF compared to wild-type; transcripts for Notch1 target genes, such as *Hes-1*, *Herp1*, *Herp2* (19), and *Nrarp* (20) were also reduced significantly.

The Notch family of transmembrane receptors participates in a signaling pathway controlling a broad spectrum of metazoan cell fates and developmental processes through local cell-cell interactions (21). Alteration of signaling through the Notch family of receptors can markedly affect differentiation, proliferation, and apoptotic events. Genetic ablation studies indicate that Notch1 is crucial for early development and re-growth of several tissues (22,23). Activation of the Notch pathway inhibits differentiation in different developmental contexts and has been associated with the amplification of some somatic stem cells— not only the neural (24) and

hematopoietic stem cells (25), but also hepatocyte (26,27) and intestinal epithelial stem cells (28,29). Considering the importance of the Notch1 signal cascade in developmental biology, the microarray observations indicated the possibility that Nrf2 could be a key molecule affecting both embryonic and adult tissue stem cell renewal as well as cell fates. This study characterizes the effects of *Nrf2* genotype on the expression of *Notch1* and its effector genes and the importance of Nrf2-Notch1 crosstalk in liver regeneration.

Results

Expression of Notch1 and its effector genes are decreased in Nrf2-null MEFs

Microarray analyses compared gene expression patterns in wild-type or *Nrf2*-disrupted mice in order to identify Nrf2-regulated genes (13) and provided hints for interactions between Nrf2 and other signaling pathways such as the aryl hydrocarbon receptor (AhR) (30) and nuclear factor- κ B (NF- κ B) pathways (31). Further analysis of one of these data sets (30) revealed that *Notch1* transcript levels were 14-fold lower in *Nrf2*-null compared to wild-type MEFs. Furthermore, the expression of *Hes-1* and *p21*, two downstream genes in the Notch1 pathway (19,32), were also reduced substantially in *Nrf2*-null cells. To confirm the microarray data indicating that Nrf2 promotes the Notch1 signaling pathway, we analyzed the expression of additional downstream effector genes by semi-quantitative reverse transcriptase-polymerase chain reaction (RT-PCR) in wild-type and *Nrf2*-null MEFs. We found that the abundance of transcripts for the Notch1 target genes *Hes-1*, *Herp1*, *Herp2*, *Nrarp*, and *p21* were also reduced in *Nrf2*-null MEFs, corresponding to the reduced *Notch1* expression. By contrast, no effect on the abundance of transcript for the Notch1 ligand, *Jag1*, was observed (Fig. 1A). Quantitative real-time RT-PCR analysis confirmed the reduction in *Notch1* expression in *Nrf2*-null mice (Fig. 1B). We also found that expression of a prototypic Nrf2-regulated gene, *Gsta1*, was substantially lower in the *Nrf2*-deficient fibroblasts. Expression of *Gsta1* was induced by treatment with 2.5 μ M sulforaphane (an activator of Nrf2 signaling) (14) in wild-type cells only (Fig. 1B). As with *Gsta1*, induction of *Notch1* by sulforaphane was also lost in the absence of functional Nrf2 (Fig. 1B). These results suggest a role for Nrf2 in *Notch1* expression.

Notch1 expression is influenced by Nrf2 abundance in mice

To elucidate whether the effect of *Nrf2* genotype on *Notch1* expression observed in MEFs also occurred in vivo, transcript abundance was assessed in adult livers. *Notch1* transcripts were consistently reduced ~ 40% in livers of adult *Nrf2*-null mice compared to those in wild-type mouse livers (Fig. 1C and supplemental Fig. 1B). *Keap1*-null mice, which exhibit constitutive activation of the Nrf2 pathway, die by 3 weeks of age from malnutrition through formation of esophageal stricture (33). This knockout mouse can be rescued by reducing the function of Nrf2 through genetic engineering. To analyze the effect of Nrf2 on *Notch1* expression in adult mice, *Notch1* transcripts were measured in livers of 8-week old male mice of three genotypes: *Keap1*^{-/-}::*Nrf2*^{+/-}, *Keap1*^{+/-}::*Nrf2*^{+/-}, and *Keap1*^{+/-}::*Nrf2*^{-/-}. Although the mice of these three genotypes survive, the amount of functional Nrf2 differs among the genotypes. In the *Keap1*-deficient mice, which partially or completely lack this repressor of Nrf2, Nrf2 activity is higher in *Keap1*^{-/-}::*Nrf2*^{+/-} than in *Keap1*^{+/-}::*Nrf2*^{+/-} mice (33,34). Nrf2 is absent in *Keap1*^{+/-}::*Nrf2*^{-/-} mice. The order of abundance of hepatic Nrf2 is *Keap1*^{-/-}::*Nrf2*^{+/-} > *Keap1*^{+/-}::*Nrf2*^{+/-} > *Keap1*^{+/-}::*Nrf2*^{-/-}. *Notch1* expression exhibits the same qualitative pattern by genotype, as does expression of two other Nrf2 target genes *Nqo1* and *Gsta1* (Fig. 1C and supplemental Fig. 1C). Thus, the magnitude of Nrf2 signaling appears to affect the extent of *Notch1* expression.

Functional ARE in the gene-regulatory region of Notch1

We investigated the possibility that *Notch1* is a direct target gene of the Nrf2 transcription factor. Sequence analysis (NCBI, mouse genome sequence viewer and (35)) revealed that the

proximal promoter region of *Notch1* bears four consensus AREs (shown as 1 to 4 in Fig. 2A). Forced expression of Nrf2 enhanced the activity of the -1640 *Notch1* luciferase reporter gene (Fig. 2B) in MEF cells. Also, in accord with the observations in MEF cells, treatment with sulforaphane significantly increased *Notch1* reporter activity, both in the absence and presence of exogenous Nrf2. Thus, Nrf2 appears to directly affect *Notch1* expression in MEFs and this is likely mediated by binding of Nrf2 to regulatory domain(s) in the -1640 proximal promoter of *Notch1*.

To elucidate whether and where any functional enhancer regions of the *Notch1* are located, serial deletion reporter constructs bearing the *Notch1* 5 μ -flanking region were transfected into both wild-type MEF and the P19 embryonal carcinoma cell line, in which *Notch1* is abundantly expressed within differentiation (36). We identified the region from -315 to -189 as the positive regulatory region in both cell types (Fig. 2C). One consensus ARE core sequence (1-ARE), TGABNNNGC (B=C, G, T, N=A, T, G, C) (1), was present in the region -204 to -196. To elucidate whether the 1-ARE was functional, we created p-206 and point mutant reporter genes (Fig. 2D) and transfected them into MEFs. Co-expression of Nrf2 with p-206 led to a 4-fold enhancement in reporter activity compared to that in vector-transfected cells (Fig. 2D). The responsiveness of a p-206 mutant ARE (mARE) luciferase reporter to Nrf2 was reduced compared to the wild-type p-206 reporter. These results suggest that the 1-ARE in the *Notch1* gene regulatory region is a functional *cis*-element in MEFs.

We performed a series of electrophoretic mobility shift assays (EMSAs) to determine whether the positive regulatory element directly binds transcriptional factors. There are three major Cnc candidates for binding to AREs and stimulating gene expression: Nrf1, Nrf2, and Nrf3 (37). Nrf3 was considered the least likely molecule because of its low expression among the three candidates in MEFs. Neither *Nrf1* nor *Nrf3* gene expression was altered in the wild-type compared to *Nrf2*^{-/-} MEFs (supplemental Fig. 1A). We considered Nrf2 the strongest candidate on the basis of the comparison of *Notch1* expression in *Nrf2*-null versus wild-type MEFs. To determine whether Nrf2 formed a complex with 1-ARE from the *Notch1* gene regulatory region, we prepared recombinant Nrf2 and its binding partner, small MafK. Neither Nrf2 alone nor MafK alone bound the *Notch1*-ARE (Fig. 2E, left). Formation of the heterodimeric complex (Nrf2-MafK) bound to the *Notch1* 1-ARE only occurred when both proteins were added (Fig. 2E, right). The intensities of the bands representing complex formation using both recombinant proteins were reduced by the addition of a cold competitor oligonucleotide, the ARE from *Gsta1*, but not by a point mutant oligonucleotide of the *Notch1* 1-ARE. Thus, *Notch1* 1-ARE has *cis*-element potential for Nrf2-MafK heterodimer binding.

The 1-ARE formed complexes when incubated with nuclear extracts from MEFs (Fig. 2F). The band indicating the binding complex disappeared following addition of the *Gsta1*-ARE as a competitor, but not in the presence of excess mutant *Notch1* 1-ARE (Fig. 2F). An EMSA conducted with an antibody to Nrf2 showed supershifted bands from the complex; however, we did not observe supershift or disappearance of the bands in the presence of an antibody to Nrf1 (Fig. 2G). To determine if basal *Notch1* expression is stimulated by Nrf2 through 1-ARE in MEFs, we performed a chromatin immunoprecipitation (ChIP) assay with wild-type and *Nrf2*^{-/-} MEFs. Under stringent conditions in which the positive control *Gsta1*-ARE locus (38) was barely detectable, the antibody to Nrf2 precipitated the proximal region of the *Notch1* promoter, including 1-ARE, in nuclear extracts from wild-type, but not *Nrf2*^{-/-}, MEFs. Collectively, the promoter reporter, EMSA, and ChIP results indicate that Nrf2, likely in complex with other bZip transcription factors such as the small Mafs, form a complex with the 1-ARE of the *Notch1* gene regulatory region.

Activation of Notch1 expression in *Rosa^{CreER/CreER}::Keap1^{flox/flox}* MEFs

In the *Keap1^{-/-}* liver, Nrf2 accumulates in the nucleus due to impaired Keap1-mediated Nrf2 degradation. We found that the amount of *Notch1* transcripts was increased in *Keap1^{-/-}* P1 liver (supplemental Fig. 1D). However, the constitutively active status of Nrf2 may produce indirect effects on gene expression. Indeed, these *Keap1^{-/-}* mice do not survive more than 3 weeks (33). To avoid such constitutive Nrf2 activation and toxicity, we isolated conditional Nrf2-activating MEFs (RCKF) from *Rosa^{CreER/CreER}::Keap1^{flox/flox}* mice as well as control MEFs (RC) from *Rosa^{CreER/CreER}* mice. *Keap1* was disrupted in RCKF cells exposed to 4-hydroxytamoxifen (4-OHT), but not when exposed to vehicle (Fig. 3A). In control RC MEFs, 4-OHT did not induce *Notch1* expression or that of *Nqo1*, a representative Nrf2 target gene (Fig. 3B). Thus, 4-OHT does not itself influence Nrf2-related gene expression. Expression of both *Nqo1* and *Notch1* was induced in RCKFs treated with 4-OHT (Fig. 3B), and this was accompanied by the accumulation of Nrf2 (Fig. 3C), and disruption of *Keap1* (Fig. 3A). Thus, alteration of the abundance of cellular Nrf2 directly influenced the abundance of *Notch1* transcripts.

Reduced Notch1 signal transduction in Nrf2 null MEFs

We developed a co-culture model to determine whether downstream Notch1 signaling was affected by *Nrf2* genotype. *Nrf2*-disrupted or wild-type MEFs were each co-cultured with clones of human embryonic kidney 293 (HEK293) cells stably over-expressing Notch1 ligands (human DLL1 and human JAG1), which served as pathway activators (Fig. 4). We assessed the amount of the exogenous Notch1 ligands JAG1 and DLL1 in the HEK293 cells by immunoblot analysis (Fig. 4A). To evaluate the activity of the Notch1 pathway, we monitored the expression of the direct Notch1 target genes *Hes-1*, *Herp1*, *Herp2*, and *Nrarp*. When wild-type MEFs were co-cultured with J1 or J2 HEK293 cells, both of which stably express human Jag1 protein, we observed a significant increase in the expression of the Notch1 target genes compared to that in co-cultures with clone 3 of mock-transfected HEK293 cells. Similar fold induction of *Hes-1*, *Herp1*, *Herp2*, or *Nrarp* was seen when the J1 or J2 lines were co-cultured with *Nrf2^{-/-}* MEFs, although absolute expression was considerably lower than in wild-type MEFs. With the DLL1-expressing, D2 stable clone, *Hes-1* transcripts were clearly increased in co-cultures with wild-type MEFs, but showed a dampened response in co-cultures with *Nrf2*-null MEFs (Fig. 4C). *Herp1*, which is another direct target gene of Notch1, also exhibited increased transcript abundance in wild-type, but not *Nrf2*-null MEFs co-cultured with DLL1-overexpressing HEK293 cells. Thus, *Nrf2*-null MEFs show significantly decreased Notch responses.

Delayed regeneration of the liver after partial hepatectomy and diminished Notch1 signaling in *Nrf2^{-/-}* mice

Notch signaling is essential during embryogenesis of mice. Conditional gene targeting studies have revealed that Notch signaling is also important after birth, as well as in adult mice (39, 40). Notch1 is activated and plays an important role in cell proliferation during liver regeneration after partial hepatectomy. Liver injection of silencing RNA for Notch1 or Jag-1 prior to partial hepatectomy, significantly suppresses the proliferation of hepatocytes at days 2 to 4 of the regenerative response (26). Liver regeneration from partial hepatectomy is also delayed in *Nrf2*-disrupted mice compared to that in wild-type mice (41). We confirmed this delayed liver regeneration at 72 hr after partial hepatectomy in *Nrf2*-null mice (Fig. 5B). We hypothesized that this delay was associated with altered *Notch1* expression and signaling in the *Nrf2*-disrupted mice. To verify this hypothesis, we performed two-thirds partial hepatectomy (both median and left lobes) in *Nrf2*-null mice and measured the transcription of the Notch1 target gene *Hes1* to evaluate the impact on Notch1 signaling (Fig. 5A). At 30 min after partial hepatectomy, the abundance of transcripts for *Nqo1*, which reflects Nrf2 activity,

and *Hes1*, which reflects Notch1 signaling, was similar in livers of mice of each genotype to the abundance prior to hepatectomy (supplemental Fig. 2). However, at 3 hr after partial hepatectomy, there were increases in transcripts encoding the Notch1 ligands (*Jag1* and *Dll1*) in livers of both genotypes (Fig. 5A). The abundance of the Notch1 transcript in livers of *Nrf2*^{-/-} mice was less than the abundance in livers from wild-type mice, and the *Nrf2*^{-/-} mice failed to induce Notch1 6 hours following partial hepatectomy (Fig. 5B). *Hes1* transcripts were more abundant in the livers of wild-type mice compared to the amount in livers of *Nrf2*^{-/-} mice. Although the fold induction of *Hes1* was similar between genotypes, absolute levels of *Hes1* transcripts were lower following partial hepatectomy in *Nrf2*^{-/-} mice (Fig. 5B). The amount of basal *Nqo1* transcripts was also reduced in the *Nrf2*-null mice and the induction in response to partial hepatectomy was completely blocked. In the livers of sham-operated mice, the abundance of transcripts for the direct partner of Notch1 (*Rbpj*) for the activation of the target genes was not different in the livers of *Nrf2*^{-/-} mice compared to that in the wild-type mouse livers, and the abundance of these transcripts decreased 6 hours after partial hepatectomy only in the *Nrf2*^{-/-} mice (Fig. 5B). This result suggests that the different responses of *Nqo1* (absence of induction) and *Hes1* (reduced induction) to partial hepatectomy between wild-type and *Nrf2*-null mice are caused by differences in initial amounts of Nrf2 and Notch1 proteins in the liver. Absence of Nrf2 in the liver seemed to affect Notch1 signaling in early phase of regenerative process after 2/3 partial hepatectomy due to the lower basal transcript abundance of *Notch1* in the *Nrf2*-null mice.

Hepatocyte-specific expression of the Notch intracellular domain rescued the delayed regeneration of the liver after partial hepatectomy in *Nrf2*-null mice

To restore Notch1 signaling in the hepatocytes in the livers of *Nrf2*^{-/-} mice, triple compound *Nrf2*^{-/-}::*Rosa*^{NICD/-}::*AlbCre* mice were established by crossing *Nrf2*-null mice with *Rosa*^{NICD/-} or *AlbCre* transgenic mice in a step-by-step manner. Only in this composite line of mice is the Notch intracellular domain (NICD), which is the transcriptionally active Notch1 cleavage fragment, and enhanced GFP (EGFP) in hepatocytes present due to the removal of the transcriptional stop signal sequence placed between both loxP sequences directly downstream of the Rosa 26 promoter region by the specific expression of Cre recombinase controlled by the albumin enhancer promoter (Fig. 6A). Homologous recombination in the Rosa 26 locus (Cre-active) leading to expression of NICD was only detected in the DNA isolated from the liver of *Nrf2*^{-/-}::*Rosa*^{NICD/-}::*AlbCre* mice (Fig. 6B). Both NICD and EGFP were only present in the triple compound mice, detected by immunoblot analyses of whole liver extracts (Fig. 6C). The abundance of transcripts for the Notch1 direct target gene *Hes1* were increased in the *Nrf2*^{-/-}::*Rosa*^{NICD/-}::*AlbCre* mice compared to the other two lines of mice (Fig. 6D). Thus, this triple compound line exhibited enhanced Notch1 signaling in hepatocytes. Two-thirds partial hepatectomies were conducted using this line and two sets of control lines, *Nrf2*^{-/-}::*Rosa*^{NICD/-} and *Nrf2*^{-/-}::*AlbCre*. There were no significant differences among three genotypes in the size of livers in animals undergoing sham partial hepatectomy (Fig. 6E). But, following partial hepatectomy, the *Nrf2*^{-/-}::*Rosa*^{NICD/-}::*AlbCre* line showed enhanced regeneration of liver weight comparable to that seen in wild-type mice (Fig. 6E, compare with Fig. 5B). Neither of the control lines (*Nrf2*^{-/-}::*Rosa*^{NICD/-} or *Nrf2*^{-/-}::*AlbCre*) influenced the delayed regeneration rate typical of the *Nrf2*-null mice. These results demonstrate that constitutive expression of the gene encoding Notch1 and Notch1 signaling are supported by Nrf2 and contribute to tissue regeneration.

Discussion

We provide several lines of evidence indicating that Nrf2 enhances the expression of the gene encoding Notch1 and the amplitude of its downstream signals (Fig. 1). First, a comparison of expression profiles in MEFs isolated from wild-type and *Nrf2*-disrupted mice showed that

Notch1 expression was dampened in the *Nrf2*-null cells. Additionally, transcripts for downstream effectors of Notch1, *Hes-1*, *Herps*, *Nrarp*, and *p21*, were also diminished in the knockout cells. Second, the Notch1 target genes were induced by treatment of wild-type, but not *Nrf2*-knockout cells, with the chemopreventive agent sulforaphane, a known activator of Nrf2 signaling. Third, genetic manipulation of the abundance of Nrf2 in mouse liver-- by disruption of the genes encoding Nrf2 and its repressor, Keap1-- demonstrated a dose-dependent association between magnitude of Nrf2 signaling and *Notch1* expression. *Notch1* expression was decreased in the livers of *Nrf2*-null mice, but was enhanced in *Keap1*^{-/-}::*Nrf2*^{+/-} mouse livers, which is similar to the expression of prototypic Nrf2-regulated genes *Gsta1* and *Nqo1* in these genotypic settings. Although the *Keap1*^{-/-}::*Nrf2*^{+/-} mice exhibit a constitutive activation of Nrf2, these animals do not exhibit the pre-weaning lethal phenotype of *Keap1*-null mice.

The co-culture experiments with HEK293 cells overexpressing the Notch1 ligands JAG1 or DLL-1 indicated that decreased expression of *Notch1* in *Nrf2*-null MEF directly impaired Notch1 signal transduction, as reflected in reduced expression of its target genes *Hes-1*, *Herps*, and *Nrarp*. Thus, Notch1 signaling is limited by the abundance of Notch1, which is transcriptionally controlled by Nrf2, not by the abundance of the Notch1 ligands. This ligand-Notch1 interaction may mimic events early in tissue regeneration after injury. Partial hepatectomy provides a model to examine signaling pathways involved in the response to hepatic injury. Prior studies have shown that Notch1 signaling increases rapidly following partial hepatectomy (26), and that liver regeneration is delayed in *Nrf2*-null mice (41), an observation that we confirm here. Köhler et al. (26) observed that nuclear translocation of NICD increased and peaked within 15 minutes after partial hepatectomy in rats, indicating activation of Notch signaling. In the same study, expression of the Notch-dependent target gene *Hes1* increased within 30 to 60 minutes. We report that at 6 hr after partial hepatectomy no change in abundance of *Notch1* and *Nrf2* transcripts was observed, but *Hes1* transcripts, as well as those encoding the Notch1 ligands Jag1 or Dll-1, were increased. Although we observed similar relative increases of *Hes1* transcripts in the livers of *Nrf2*-null mice following partial hepatectomy, the absolute amount was only one-third of that in wild-type mice. This phenomenon was similar to the observations in the in vitro co-culture system using MEFs. Because the abundance of the transcripts of the Notch1 ligands did not appear to be influenced by *Nrf2* genotype following partial hepatectomy, the differential upregulation of *Hes1* by genotype may reflect abundance of Notch1 protein. Notch1 signaling, which is supported by Nrf2, appeared to influence early steps in liver regeneration and we tested this by creating *Nrf2*^{-/-}::*Rosa*^{NICD}^{-/-}::*AlbCre* mice, in which have NICD is produced in specifically in hepatocytes in the *Nrf2*- null background. Forced hepatic Notch1 signaling mediated by NICD rescues the phenotype of delayed liver regeneration observed in the *Nrf2*-null mice.

Other effects of Nrf2 on Notch1 signaling can be envisioned. *Nrf2*-null mice do not show any growth and development phenotypes under normal conditions, either in early development or postnatally (3,42). By contrast, *Notch1* disruption is lethal to mice at around embryonic day 10.5 (E10.5), indicating that this gene and its signals are essential in embryonic development stage before E10.5 (21). The *Nrf2* transcript is detected at this time only in the central nervous system by RNA in situ hybridization and this is the earliest point of detection (43). Thus, Notch1 is likely present before Nrf2 (Gene Expression Data from MGI), suggesting that expression of *Notch1* in early development does not depend on Nrf2. Alternatively, considering *Nrf1* expression patterns during embryonic development and the embryonic lethal phenotype of *Nrf1*-disrupted mice, Nrf1 may substitute for Nrf2 to support *Notch1* expression through the 1-ARE early in life. Further analyses are required to elucidate how ARE-containing genes are regulated by Nrf2, Nrf1, or other factors during embryogenesis.

Nrf2-mediated regulation of *Notch1* expression may be most critical in postnatal stages, rather than during development when *Notch1* is likely regulated by other factors, because Nrf2 disruption does not produce altered phenotypes during early development stages. Nrf2 is abundant in liver, kidney, lung, and the gastrointestinal-tract, tissues that also contain stem cells. *Notch* and *Notch*-related gene expression also occur in these tissues (26,28,29,44,45). In such tissues, damaged cells must be replaced by newly differentiated cells for routine tissue maintenance. Furthermore, many of these tissues face the highest burdens from environmental exposures to toxicants and resultant tissue injury. The Keap1-Nrf2 pathway regulates a well described adaptive response that reduces macromolecular damage, following exposure to conditions that increase the amounts of free radicals and electrophiles, through stimulation of genes encoding antioxidative and electrophile detoxication enzymes (4). Nrf2 signaling also stimulates pathways affecting the recognition, repair, or removal, or all of these, of damaged macromolecules, notably proteins and DNA (38). Our previous work indicates that repair of tissue damage represents a third component of the adaptive cytoprotective response controlled by Nrf2. *Nrf2*-null mice are considerably more sensitive to hyperoxic lung injury (46). Treatment of mice with the triterpenoid Nrf2 activator CDDO-Imidazolide during, but not before hyperoxic exposure, led to substantial protection against the biochemical and morphological sequelae of acute lung injury and appeared to enhance tissue remodeling (47). The current study indicates that Nrf2 facilitates tissue regeneration in the liver by regulating *Notch1* expression. With these diverse actions influencing the cellular response to toxins or tissue damage, strategies using drugs or foods to enhance Nrf2 signaling and that of its interacting networks provide multifaceted opportunities for disease prevention.

Materials and Methods

Mice and Genotyping

Keap1^{+/-} mice were back-crossed more than 10 times with C57BL/6J mice purchased from the Jackson Laboratory. *Nrf2*^{-/-} mice, which were back-crossed more than 20 times into a C57BL/6J background, were a gift from Dr. Ken Itoh (Hirosaki University). *Keap1-Nrf2* compound knockout mice were established by mating *Keap1*^{+/-} with *Nrf2*^{+/-} mice to generate *Keap1*^{+/-}::*Nrf2*^{+/-} mice. Each compound genotype was obtained from matings between *Keap1*^{+/-}::*Nrf2*^{+/-} mice (33). *Keap1*^{flox/+} mice were generated as described previously (8). *Gt(ROSA)26Sor^{tm1(Cre/Esr1)Nat}* mice (*Rosa*^{CreER/CreER}) (48), *Gt(ROSA)26Sor^{tm1(Notch1)Dam1J}* (*Rosa*^{NICD/-}) (49) and *B6.Cg-Tg(Alb-cre)21Mgn/J (AlbCre)* (50) were obtained from the Jackson Laboratory. *Keap1*^{flox/flox}::*Rosa*^{CreER/CreER} mice were established by matings with *Keap1*^{flox/+} and *Rosa*^{CreER/CreER} mice in consecutive steps. *Nrf2*^{-/-}::*Rosa*^{NICD/-}::*AlbCre* mice resulted from crossings with *Nrf2*^{-/-}::*Rosa*^{NICD/NICD} and *Nrf2*^{-/-}::*AlbCre* mice, which were established by the consecutive mating of *Nrf2*^{+/-}::*AlbCre* and *Nrf2*^{+/-}::*Rosa*^{NICD/-} mice. All mice were genotyped by previously reported methods (8,33,48) or by PCR described in the table S2. All animal breeding and handling was conducted in accordance with protocols approved by the Animal Care and Use Committee of the Johns Hopkins Medical Institutions.

Partial Hepatectomy

Male mice (9- to 10-week old) were placed into a plexiglass chamber for induction of anesthesia with 2% isoflurane and 2 liter/min oxygen flow. After primary anesthetization, they were maintained under anesthesia by isoflurane inhalation through a suitable mouthpiece. The left and median lobes of the liver were pushed out from an incision just under the xiphoid process and were removed with a ligature (51). Following surgery, mice were returned to their cages and given free access to food and water. Sham-operated control animals were treated in an identical fashion with the omission of hepatectomy.

Cell Culture

MEFs were established from the embryos of *Nrf2*-null or wild-type littermates. On day 14.5 of pregnancy, mice were sacrificed and embryos removed from the uterus. Extra-embryonic tissues were removed from individual fetuses, followed by rinsing in PBS to remove any blood. Embryos were decapitated and eviscerated using sterile forceps. A portion of the tail was used as a source of DNA for genotype and gender confirmation (52) by PCR. The carcasses were transferred to a sterile conical centrifuge tube containing PBS and rinsed by inverting twice. The carcasses were dissociated by finely mincing with a scalpel blade, then pressing through a sterile cell strainer with forceps. They were rinsed on the screen twice with a 0.05% trypsin solution, transferred to a small culture flask, and stirred gently in a humidified 5% CO₂ incubator at 37°C for 30 minutes. Suspended cells were decanted and collected by centrifugation. Cell pellets were washed twice with 30 ml Iscove's MEM (Invitrogen, USA) containing 10% fetal bovine serum (FBS) (Invitrogen, USA) (MEF growth medium). Cells were plated on dishes in MEF growth medium; 24 hr later the cells were rinsed with PBS/0.02% EDTA twice and the medium was replaced with fresh MEF growth medium. In approximately 2–4 days, the cultures were confluent and expanded for use in experiments and for making frozen stocks. MEFs derived from male embryos were used in all experiments. P19 cells (ATCC) were grown as monolayers and maintained in α -minimum essential medium (Sigma, USA), containing 10% fetal bovine serum, and incubated at 37°C in a humidified atmosphere of 5% CO₂. To establish human Jagged1 or human Delta-like 1 expressing cells, *pLZRShJagged1* or *pLZRhDl1* (53), provided by Dr. Leonor Parreira (University of Lisbon), were transfected into HEK293 cells. Simultaneously, negative-control transfectant, which was transfected with *LZRSpBMN-linker-IRES-EGFP* as a mock vector, was also prepared. After 2 weeks of selection with 10 μ g/ml puromycin, several single resistant colonies were picked and maintained in each dish using Iscove's MEM containing 10% FBS with 8 μ g/ml puromycin. RCKF and RC MEFs were isolated from embryos of *Rosa^{CreER/CreER}; Keap1^{fllox/fllox}* or *Rosa^{CreER/CreER}* pregnant mice (ED14.5), respectively. Each MEF culture was established from single embryos. Experiments were conducted within passage number 5. 4-Hydroxy-tamoxifen (4-OHT, Sigma, USA) was dissolved in 100% ethanol at 10 mM. RCKF and RC were analyzed after 3 days-repetitive exposure to conditioned media that included 1 μ M 4-OHT.

Co-Culture Assay for Notch Signaling

Cells expressing the Notch1 ligand or negative control cells (5×10^5) were spread in 10-cm dishes 4 days before co-culture with *Nrf2*-null or wild-type MEFs. *Nrf2*-null or wild-type MEF were plated at 4×10^5 cells/dish. Notch ligand-expressing cells or control cells were collected with PBS/EDTA (final 0.02% EDTA) and washed once before seeding. The transfectants were split into dishes of each MEF genotype, containing complete medium and incubated at 37°C, 5% CO₂. Total RNA was isolated and analyzed by RT-PCR. It was confirmed that the primer set only amplified products from MEF under our PCR conditions.

Protein Preparation and Immunoblot Analyses

Proper size-cut tissues were homogenized in RIPA-I buffer, which contained a protease inhibitor cocktail (Roche, USA). Cultured cells were harvested with RIPA-I buffer directly. An equal volume of 2xSDS sample buffer was added and the samples were denatured by boiling for 5 min. Samples were applied to SDS-PAGE and transferred to an Immobilon PVDF membrane (Millipore, USA). The membranes were blocked with Tris-buffered saline with 0.05% Tween 20 and 5% skim milk and then treated with a primary antibody. The preparative membranes were reacted with appropriate secondary antibodies conjugated to horseradish peroxidase (Invitrogen Zymed, USA). The immunocomplexes were visualized with ECL (GE-Healthcare, USA). The specific antibodies for Lamin B1 (sc-6216), EGFP (sc-8334), Jagged-1

(sc-8303), and Delta-1 (sc-9102) were obtained from Santa Cruz Biotechnology. Antibodies for Cre recombinase (ab24608) and NICD (07-1232) were purchased from Abcam and Millipore, respectively. The monoclonal antibody against Nrf2 used for immunoblotting was a gift from Dr. Ken Itoh (Hirosaki University).

Oligonucleotide Microarray

Total RNA was purified using the RNeasy Mini kit (Qiagen, USA) after isolation using TRIzol (Invitrogen, USA) according to the manufacturer's instructions. Murine Genome MOE 430A GeneChip arrays (Affymetrix, USA), which contain probes for detecting ~14,500 well-characterized genes and 4371 expressed sequence tags were used to probe the gene expression in MEFs as described previously (12). Scanned output files were analyzed using Affymetrix GCOS (GeneChip Operating Software) and independently normalized to an average intensity of 500 before comparison.

Notch1 Reporter Constructs

The mouse *Notch1* gene regulatory region (−2 kb) from the major transcripts including the initiation codon sequence was isolated from C57BL/6J mouse liver genomic DNA by PCR. The region was directly cloned between *Bgl* II and *Nco* I sites in *pGL3 basic* (Promega, USA) and confirmed by sequence analysis. In this construction, the ATG of *Notch1* was replaced with the ATG of luciferase cDNA. Serial promoter deletion fragments were prepared by the *S1-Exo*III nuclease reaction method followed by *Nco* I digestion. Then, the fragments were ligated to the site between *Ecl* 136II and *Nco*I sites of *pGL3 basic*. Serial point mutant and p-206 constructs were produced by PCR primer site-directed mutagenesis. Primers are shown in table S1. All constructs were confirmed by sequencing. Because *pRLTK* (Promega, USA) bears an ARE sequence in the thymidine kinase-promoter region, this ARE sequence was deleted in order to use this vector for normalizing transfection efficiency. The improved normalizing vector, *pRLTK-ΔARE*, was constructed by deleting the *Sma* I and *Pvu* II fragment from *pRLTK*. Constructs used in transfection experiments were purified with Qiagen plasmid kits (Qiagen, USA) and detoxinized with an endotoxin removal kit (Mirus Bio Corp., USA).

Serial Deletion Reporter Assay

MEFs or P19 cells were plated at a density of 2×10^5 cells/60-mm dish 24 hr before DNA transfection. An equimolar concentration of the DNA of each construct (10 μ g = 4.3 pmol of each reporter gene and 0.5 μ g of *pRLTK-ΔARE*) was introduced into the cells by calcium phosphate co-precipitation (54). Transfections were repeated three to six times with independent plasmid DNA preparations. *pBR322* plasmid DNA was used as a carrier to adjust the total amount of DNA. Cells were harvested 48 hrs after transfection. Luciferase activity was measured according to the manufacturer's instructions (Promega, USA) and normalized to Renilla luciferase activity derived from *pRLTK-ΔARE*. Sulforaphane (LKT Labs, MN) was used as an inducer of ARE-regulated genes (55). For *trans*-activation assays, 4 μ g of the reporter gene was transfected together with 8 μ g *pCMVnrf2* and 0.5 μ g *pRLTK-ΔARE* normalizing vector.

Isolation and Purification of Total RNA and RT-PCR

Cells were seeded at 60% confluence the day before treatment with vehicle or sulforaphane. Total RNA was prepared from MEFs or P19 cells using Trizol (Invitrogen, USA) or Isogen (Wako, USA), and then, total RNA was purified using the RNeasy mini kit (Qiagen, USA). Mouse livers were perfused with ice-cold PBS prior to isolation of total RNA using the Versagene RNA purification system (Gentra Systems, USA). RNA quality was confirmed by electrophoresis before reverse-transcriptase (RT) reaction. Several genes were analyzed by SYBR green real time quantitative RT-PCR, and representative differentiation marker genes

were analyzed by semi-quantitative RT-PCR. cDNA was synthesized using the iScript system (BioRad, USA). Real-time PCR was performed on a Bio-Rad My-IQ real-time PCR machine using Applied Biosystems SYBR green PCR master mix in triplicate 20 μ l reaction volumes. The PCR efficiency was determined from a standard curve and used the Pfaffl method for calculation of fold changes (56). Melt curves and agarose gel electrophoresis were employed to ensure specificity of amplified product. Primers are shown in table SI. The intensity of bands was measured with ImageJ analysis software provided from NIH.

Analysis of DNA-Nuclear Factor Binding

Nuclear extracts were prepared from MEF and P19 cells according to Dignum *et al* (57). Protein concentrations of each nuclear extract were determined by the BioRad protein assay using IgG as the standard. Probes were prepared by end labeling 20 ng of the primary strand oligonucleotide with [γ - 32 P] ATP by T4 polynucleotide kinase, which were annealed subsequently to the complementary oligonucleotide. For the standard electrophoretic mobility shift assay (EMSA), 25 μ l reaction mixture containing approximately 2×10^4 cpm of probe nucleotide was incubated with 20 μ g protein of the nuclear extract in a buffer consisting of 10 mM HEPES (pH 7.9), 25 mM KCl, 1 mM EDTA, 1 mM ZnCl₂, 1 mM dithiothreitol, 0.5 mM phenylmethylsulfonyl fluoride, 4 μ g poly(dI-dC), 0.05% Nonidet P-40, and 10% glycerol at 4°C for 30 min. For the competition experiments, each competitor oligonucleotide (table S1) was also added to the standard EMSA reaction mixture at a 25, 50, or indicated-fold molar excess to the probe, containing approximately 2×10^4 cpm, and the final volume was adjusted to 25 or 30 μ l. The reaction products were loaded onto a 5.0% or 8.0% poly-acrylamide gels and run at 20 mA for 1.5 h in $0.5 \times$ TBE (Tris-borate-EDTA buffer, 45 mM Tris-borate and 1 mM EDTA) at 4°C. All EMSA experiments were repeated three times utilizing nuclear extracts from MEF and P19 cells treated or untreated with 2.5 μ M sulforaphane. Gels were dried and exposed to X-ray film at -80°C for 12 hr. In the case where recombinant Nrf2 and small MafK protein was used, the EMSA was performed as described previously (3).

Chromatin Immunoprecipitation (ChIP) Assay

Formaldehyde cross-linking and chromatin fragmentation were performed as described previously (30). Diluted chromatin solution was incubated with an antibody to Nrf2 (H-300: sc-13032X, Santa Cruz Biotechnology, USA), nonspecific immunoglobulin G (normal Rabbit IgG sc-2027, Santa Cruz Biotechnology, USA), or solution without antibody for 18 h at 4°C with rotation. After washing and elution, precipitated DNA was dissolved in 60 μ l of water. DNA solution (2 μ l) as a template was used for PCR with the following primers: -187mNotch1-CP: 5 μ -CTCCCTCCCGCGGCAGAGGCAC-3 μ and -257mNotch1-CP: 5 μ -CGCAGGAACCAGGGGCGGAGCC-3 μ . The primer sequences for promoters of β -Actin, which does not contain an ARE, and *Gstal*, which bears functional AREs, have been described previously (17).

Statistical Analysis

All values are expressed as mean \pm SD, except as noted otherwise. Statistical analysis was performed with unpaired Student's t-test or one-way analysis of variance (ANOVA) for comparison of multiple groups. Differences between groups were considered statistically significant when $P < 0.05$.

Supplementary Material

Refer to Web version on PubMed Central for supplementary material.

Acknowledgments

We thank Drs. H. Motohashi (Tohoku Univ.), K. Itoh (Hirosaki Univ.), S. Takahashi (Univ. of Tsukuba), M. Morita (The Salk Inst. for Biol. Studies), A. P. McMahon (Harvard Univ.), C. Murtaugh (University of Utah), I. Alcobia (Univ. of Lisboa) and L. Parreira (Univ. of Lisboa) for MafK expression vectors, anti-Nrf2 antibody, *pCaggs-nlsCre*, *pCaggs-Cre-EGFP*, *pCAGGCre-ERTM* expression vectors, genomic sequence information for *Rosa^{NICD}* mice, human Dll-1 and Jag1 expression plasmids, respectively. We also appreciate the technical assistance of Mr. Patrick Dolan, Mr. Richard Rabold, Ms. Patricia Egner, Mr. John Skoko, Drs. Miho Iijima and Hiromi Sesaki. Funding sources: This work was supported by the Maryland Cigarette Restitution Fund, NIH grants R01 CA94076, R01 HL081205, P30 ES03819, T32 ES07141, T32 CA009110 and JST-ERATO. Soona Shin is the recipient of a Samsung Scholarship (Samsung Foundation of Culture).

References

1. Motohashi H, Yamamoto M. Nrf2-Keap1 defines a physiologically important stress response mechanism. *Trends Mol Med* 2004;10:549–557. [PubMed: 15519281]
2. Rushmore TH, Morton MR, Pickett CB. The antioxidant responsive element. Activation by oxidative stress and identification of the DNA consensus sequence required for functional activity. *J Biol Chem* 1991;266:11632–11639. [PubMed: 1646813]
3. Itoh K, Chiba T, Takahashi S, Ishii T, Igarashi K, Katoh Y, Oyake T, Hayashi N, Satoh K, Hatayama I, Yamamoto M, Nabeshima Y. An Nrf2/small Maf heterodimer mediates the induction of phase II detoxifying enzyme genes through antioxidant response elements. *Biochem Biophys Res Commun* 1997;236:313–322. [PubMed: 9240432]
4. Kensler TW, Wakabayashi N, Biswal S. Cell survival responses to environmental stresses via the Keap1-Nrf2-ARE pathway. *Annu Rev Pharmacol Toxicol* 2007;47:89–116. [PubMed: 16968214]
5. Chan JY, Kwong M, Lu R, Chang J, Wang B, Yen TS, Kan YW. Targeted disruption of the ubiquitous CNC-bZIP transcription factor, Nrf-1, results in anemia and embryonic lethality in mice. *Embo J* 1998;17:1779–1787. [PubMed: 9501099]
6. Xu Z, Chen L, Leung L, Yen TS, Lee C, Chan JY. Liver-specific inactivation of the Nrf1 gene in adult mouse leads to nonalcoholic steatohepatitis and hepatic neoplasia. *Proc Natl Acad Sci US A* 2005;102:4120–4125.
7. Leung L, Kwong M, Hou S, Lee C, Chan JY. Deficiency of the Nrf1 and Nrf2 transcription factors results in early embryonic lethality and severe oxidative stress. *J Biol Chem* 2003;278:48021–48029. [PubMed: 12968018]
8. Okawa H, Motohashi H, Kobayashi A, Aburatani H, Kensler TW, Yamamoto M. Hepatocyte-specific deletion of the keap1 gene activates Nrf2 and confers potent resistance against acute drug toxicity. *Biochem Biophys Res Commun* 2006;339:79–88. [PubMed: 16293230]
9. Osburn WO, Yates MS, Dolan PD, Chen S, Liby KT, Sporn MB, Taguchi K, Yamamoto M, Kensler TW. Genetic or pharmacologic amplification of nrf2 signaling inhibits acute inflammatory liver injury in mice. *Toxicol Sci* 2008;104:218–227. [PubMed: 18417483]
10. Enomoto A, Itoh K, Nagayoshi E, Haruta J, Kimura T, O'Connor T, Harada T, Yamamoto M. High sensitivity of Nrf2 knockout mice to acetaminophen hepatotoxicity associated with decreased expression of ARE-regulated drug metabolizing enzymes and antioxidant genes. *Toxicol Sci* 2001;59:169–177. [PubMed: 11134556]
11. Beyer TA, Xu W, Teupser D, auf dem Keller U, Bugnon P, Hildt E, Thiery J, Kan YW, Werner S. Impaired liver regeneration in Nrf2 knockout mice: role of ROS-mediated insulin/IGF-1 resistance. *Embo J* 2008;27:212–223. [PubMed: 18059474]
12. Thimmulappa RK, Mai KH, Srisuma S, Kensler TW, Yamamoto M, Biswal S. Identification of Nrf2-regulated genes induced by the chemopreventive agent sulforaphane by oligonucleotide microarray. *Cancer Res* 2002;62:5196–5203. [PubMed: 12234984]
13. Kwak MK, Wakabayashi N, Itoh K, Motohashi H, Yamamoto M, Kensler TW. Modulation of gene expression by cancer chemopreventive dithiolethiones through the Keap1-Nrf2 pathway. Identification of novel gene clusters for cell survival. *J Biol Chem* 2003;278:8135–8145. [PubMed: 12506115]

14. Hu R, Xu C, Shen G, Jain MR, Khor TO, Gopalkrishnan A, Lin W, Reddy B, Chan JY, Kong AN. Gene expression profiles induced by cancer chemopreventive isothiocyanate sulforaphane in the liver of C57BL/6J mice and C57BL/6J/Nrf2 (-/-) mice. *Cancer Lett.* 2006
15. Yates MS, Kwak MK, Egner PA, Groopman JD, Bodreddigari S, Sutter TR, Baumgartner KJ, Roebuck BD, Liby KT, Yore MM, Honda T, Gribble GW, Sporn MB, Kensler TW. Potent protection against aflatoxin-induced tumorigenesis through induction of Nrf2-regulated pathways by the triterpenoid 1-[2-cyano-3-,12-dioxooleana-1,9(11)-dien-28-oyl]imidazole. *Cancer Res* 2006;66:2488–2494. [PubMed: 16489057]
16. Wakabayashi N, Dinkova-Kostova AT, Holtzclaw WD, Kang MI, Kobayashi A, Yamamoto M, Kensler TW, Talalay P. Protection against electrophile and oxidant stress by induction of the phase 2 response: fate of cysteines of the Keap1 sensor modified by inducers. *Proc Natl Acad Sci USA* 2004;101:2040–2045. [PubMed: 14764894]
17. Kwak MK, Ramos-Gomez M, Wakabayashi N, Kensler TW. Chemoprevention by 1,2-dithiole-3-thiones through induction of NQO1 and other phase 2 enzymes. *Methods Enzymol* 2004;382:414–423. [PubMed: 15047114]
18. Gao X, Talalay P. Induction of phase 2 genes by sulforaphane protects retinal pigment epithelial cells against photooxidative damage. *Proc Natl Acad Sci USA* 2004;101:10446–10451. [PubMed: 15229324]
19. Iso T, Kedes L, Hamamori Y. HES and HERP families: multiple effectors of the Notch signaling pathway. *J Cell Physiol* 2003;194:237–255. [PubMed: 12548545]
20. Weerkamp F, Luis TC, Naber BA, Koster EE, Jeannotte L, van Dongen JJ, Staal FJ. Identification of Notch target genes in uncommitted T-cell progenitors: No direct induction of a T-cell specific gene program. *Leukemia* 2006;20:1967–1977. [PubMed: 16990763]
21. Kadesch T. Notch signaling: the demise of elegant simplicity. *Curr Opin Genet Dev* 2004;14:506–512. [PubMed: 15380241]
22. Huppert SS, Le A, Schroeter EH, Mumm JS, Saxena MT, Milner LA, Kopan R. Embryonic lethality in mice homozygous for a processing-deficient allele of Notch1. *Nature* 2000;405:966–970. [PubMed: 10879540]
23. Wang XD, Shou J, Wong P, French DM, Gao WQ. Notch1-expressing cells are indispensable for prostatic branching morphogenesis during development and re-growth following castration and androgen replacement. *J Biol Chem* 2004;279:24733–24744. [PubMed: 15028713]
24. de la Pompa JL, Wakeham A, Correia KM, Samper E, Brown S, Aguilera RJ, Nakano T, Honjo T, Mak TW, Rossant J, Conlon RA. Conservation of the Notch signalling pathway in mammalian neurogenesis. *Development* 1997;124:1139–1148. [PubMed: 9102301]
25. Stier S, Cheng T, Dombkowski D, Carlesso N, Scadden DT. Notch1 activation increases hematopoietic stem cell self-renewal in vivo and favors lymphoid over myeloid lineage outcome. *Blood* 2002;99:2369–2378. [PubMed: 11895769]
26. Kohler C, Bell AW, Bowen WC, Monga SP, Fleig W, Michalopoulos GK. Expression of Notch-1 and its ligand Jagged-1 in rat liver during liver regeneration. *Hepatology* 2004;39:1056–1065. [PubMed: 15057910]
27. Jensen CH, Jauho EI, Santoni-Rugiu E, Holmskov U, Teisner B, Tygstrup N, Bisgaard HC. Transit-amplifying ductular (oval) cells and their hepatocytic progeny are characterized by a novel and distinctive expression of delta-like protein/preadipocyte factor 1/fetal antigen 1. *Am J Pathol* 2004;164:1347–1359. [PubMed: 15039222]
28. Schroder N, Gossler A. Expression of Notch pathway components in fetal and adult mouse small intestine. *Gene Expr Patterns* 2002;2:247–250. [PubMed: 12617809]
29. Fre S, Huyghe M, Mourikis P, Robine S, Louvard D, Artavanis-Tsakonas S. Notch signals control the fate of immature progenitor cells in the intestine. *Nature* 2005;435:964–968. [PubMed: 15959516]
30. Shin S, Wakabayashi N, Misra V, Biswal S, Lee GH, Agoston ES, Yamamoto M, Kensler TW. NRF2 modulates aryl hydrocarbon receptor signaling: influence on adipogenesis. *Mol Cell Biol* 2007;27:7188–7197. [PubMed: 17709388]

31. Yang H, Magilnick N, Lee C, Kalmaz D, Ou X, Chan JY, Lu SC. Nrf1 and Nrf2 regulate rat glutamate-cysteine ligase catalytic subunit transcription indirectly via NF-kappaB and AP-1. *Mol Cell Biol* 2005;25:5933–5946. [PubMed: 15988009]
32. Rangarajan A, Talora C, Okuyama R, Nicolas M, Mammucari C, Oh H, Aster JC, Krishna S, Metzger D, Chambon P, Miele L, Aguet M, Radtke F, Dotto GP. Notch signaling is a direct determinant of keratinocyte growth arrest and entry into differentiation. *Embo J* 2001;20:3427–3436. [PubMed: 11432830]
33. Wakabayashi N, Itoh K, Wakabayashi J, Motohashi H, Noda S, Takahashi S, Imakado S, Kotsuji T, Otsuka F, Roop DR, Harada T, Engel JD, Yamamoto M. Keap1-null mutation leads to postnatal lethality due to constitutive Nrf2 activation. *Nat Genet* 2003;35:238–245. [PubMed: 14517554]
34. Itoh K, Wakabayashi N, Katoh Y, Ishii T, O'Connor T, Yamamoto M. Keap1 regulates both cytoplasmic-nuclear shuttling and degradation of Nrf2 in response to electrophiles. *Genes Cells* 2003;8:379–391. [PubMed: 12653965]
35. Tsuji H I-OH, Ukai H, Katsube T, Ogiu T. Radiation-induced deletions in the 5' end region of Notch1 lead to the formation of truncated proteins and are involved in the development of mouse thymic lymphomas. *Carcinogenesis* 2003;24:1257–1268.
36. Nye JS, Kopan R, Axel R. An activated Notch suppresses neurogenesis and myogenesis but not gliogenesis in mammalian cells. *Development* 1994;120:2421–2430. [PubMed: 7956822]
37. Yu X, Kensler T. Nrf2 as a target for cancer chemoprevention. *Mutat Res* 2005;591:93–102. [PubMed: 16054659]
38. Kwak MK, Wakabayashi N, Greenlaw JL, Yamamoto M, Kensler TW. Antioxidants enhance mammalian proteasome expression through the Keap1-Nrf2 signaling pathway. *Mol Cell Biol* 2003;23:8786–8794. [PubMed: 14612418]
39. Nicolas M, Wolfer A, Raj K, Kummer JA, Mill P, van Noort M, Hui CC, Clevers H, Dotto GP, Radtke F. Notch1 functions as a tumor suppressor in mouse skin. *Nat Genet* 2003;33:416–421. [PubMed: 12590261]
40. Radtke F, Raj K. The role of Notch in tumorigenesis: oncogene or tumour suppressor? *Nat Rev Cancer* 2003;3:756–767. [PubMed: 14570040]
41. Beyer TA, Werner S. The cytoprotective Nrf2 transcription factor controls insulin receptor signaling in the regenerating liver. *Cell Cycle* 2008;7:874–878. [PubMed: 18414027]
42. Chan K, Lu R, Chang JC, Kan YW. NRF2, a member of the NFE2 family of transcription factors, is not essential for murine erythropoiesis, growth, and development. *Proc Natl Acad Sci USA* 1996;93:13943–13948. [PubMed: 8943040]
43. Gray, HF Paul A.; Luo, Ping; Zhao, Qing; Yu, Jing; Ferrari, Annette; Tenzen, Toyoaki; Yuk, Dong-in; Tsung, Eric F.; Cai, Zhaohui; Alberta, John A.; Cheng, Le-ping; Liu, Yang; Stenman, Jan M.; Valerius, M Todd; Billings, Nathan; Kim, Haesun A.; Greenberg, Michael E.; McMahon, Andrew P.; Rowitch, David H.; Stiles, Charles D.; Ma, Qiufu. *Mouse Brain Organization Revealed Through Direct Genome-Scale TF Expression Analysis. Science* 2004;306:2255–2257. [PubMed: 15618518]
44. Sander GR, Powell BC. Expression of notch receptors and ligands in the adult gut. *J Histochem Cytochem* 2004;52:509–516. [PubMed: 15034002]
45. Stanger BZ, Datar R, Murtaugh LC, Melton DA. Direct regulation of intestinal fate by Notch. *Proc Natl Acad Sci USA* 2005;102:12443–12448. [PubMed: 16107537]
46. Cho HY, Jedlicka AE, Reddy SP, Kensler TW, Yamamoto M, Zhang LY, Kleeberger SR. Role of NRF2 in protection against hyperoxic lung injury in mice. *Am J Respir Cell Mol Biol* 2002;26:175–182. [PubMed: 11804867]
47. Reddy NM, Suryanaraya V, Yates MS, Kleeberger SR, Hassoun PM, Yamamoto M, Liby KT, Sporn MB, Kensler TW, Reddy SP. The triterpenoid CDDO-imidazolide confers potent protection against hyperoxic acute lung injury in mice. *Am J Respir Crit Care Med* 2009;180:867–874. [PubMed: 19679692]
48. Badea TC, Wang Y, Nathans J. A noninvasive genetic/pharmacologic strategy for visualizing cell morphology and clonal relationships in the mouse. *J Neurosci* 2003;23:2314–2322. [PubMed: 12657690]
49. Murtaugh LC, Stanger BZ, Kwan KM, Melton DA. Notch signaling controls multiple steps of pancreatic differentiation. *Proc Natl Acad Sci USA* 2003;100:14920–14925. [PubMed: 14657333]

50. Postic C, Magnuson MA. DNA excision in liver by an albumin-Cre transgene occurs progressively with age. *Genesis* 2000;26:149–150. [PubMed: 10686614]
51. Mitchell C, Willenbring H. A reproducible and well-tolerated method for 2/3 partial hepatectomy in mice. *Nat Protoc* 2008;3:1167–1170. [PubMed: 18600221]
52. Koopman P, Gubbay J, Vivian N, Goodfellow P, Lovell-Badge R. Male development of chromosomally female mice transgenic for Sry. *Nature* 1991;351:117–121. [PubMed: 2030730]
53. Neves H, Weerkamp F, Gomes AC, Naber BA, Gameiro P, Becker JD, Lucio P, Clode N, van Dongen JJ, Staal FJ, Parreira L. Effects of Delta1 and Jagged1 on early human hematopoiesis: correlation with expression of notch signaling-related genes in CD34+ cells. *Stem Cell* 2006;24:1328–1337.
54. Chen C, Okayama H. High-efficiency transformation of mammalian cells by plasmid DNA. *Mol Cell Biol* 1987;7:2745–2752. [PubMed: 3670292]
55. Zhang Y TP, Cho CG, Posner GH. A major inducer of anticarcinogenic protective enzymes from broccoli: isolation and elucidation of structure. *Proc Natl Acad Sci USA* 1992;89:2399–2403. [PubMed: 1549603]
56. Pfaffl MW. A new mathematical model for relative quantification in real-time RT-PCR. *Nucleic Acids Res* 2001;29:e45. [PubMed: 11328886]
57. Dignam JD, Lebovitz RM, Roeder RG. Accurate transcription initiation by RNA polymerase II in a soluble extract from isolated mammalian nuclei. *Nucleic Acids Res* 1983;11:1475–1489. [PubMed: 6828386]

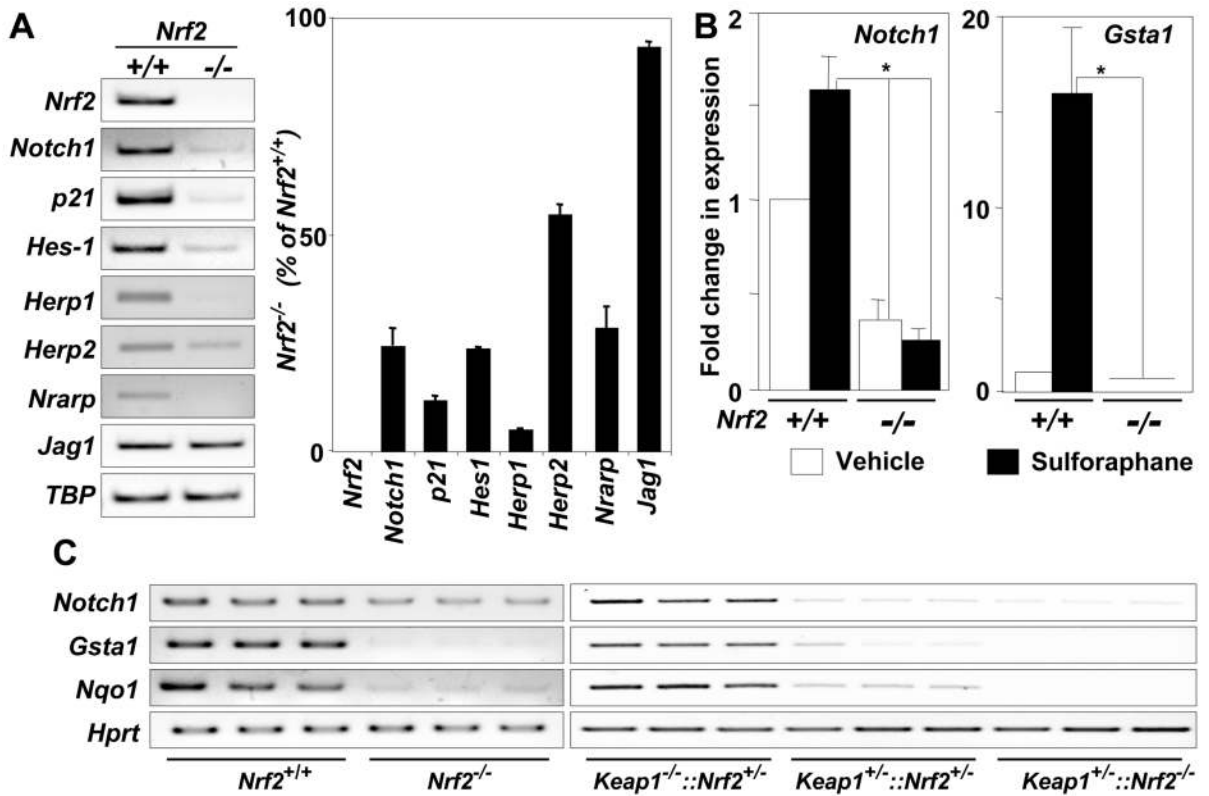


Fig. 1. Differential expression of *Notch1* and related genes in wild-type (*Nrf2*^{+/+}) and *Nrf2*-null (*Nrf2*^{-/-}) MEFs

A. Semi-quantitative RT-PCR for *Notch1*, *Notch1* effector genes (*Hes-1*, *Herp1*, *Herp2*, *Nrarp*, *p21*) and *Notch1* ligand-encoding gene, *Jag1*. The abundance of the transcript for Tata binding protein (TBP) served as a loading control. Data are quantified as the ratio of the expression of the indicated genes in *Nrf2* null/wild type. Values are the means of 3 independent experiments \pm S.E. Expression of all effector genes, except *Jag1*, was significantly lower in the *Nrf2* null MEF ($p < 0.01$; t-test). **B.** Real-time RT-PCR confirmation of changes in *Notch1* expression in wild-type versus *Nrf2*-null MEF. The loss of induction of *Gsta1*, a *Nrf2*-responsive gene, confirmed the disruption in *Nrf2* activity. MEF cultures were treated with 2.5 μ M sulforaphane or vehicle 24 h before harvesting cells for RNA isolation. Values are mean \pm S.E. * $p < 0.05$; t-test ($n=3$). **C.** RT-PCR analyses of *Notch1* and other *Nrf2* target gene expression in the livers from 8-week old *Nrf2*-null, wild-type, and various *Keap1* and *Nrf2* compound-disrupted mice. Hypoxanthine guanine phosphoribosyl transferase (*Hprt*) served as the loading control. For quantitation see supplemental Fig. 1B and 1C.

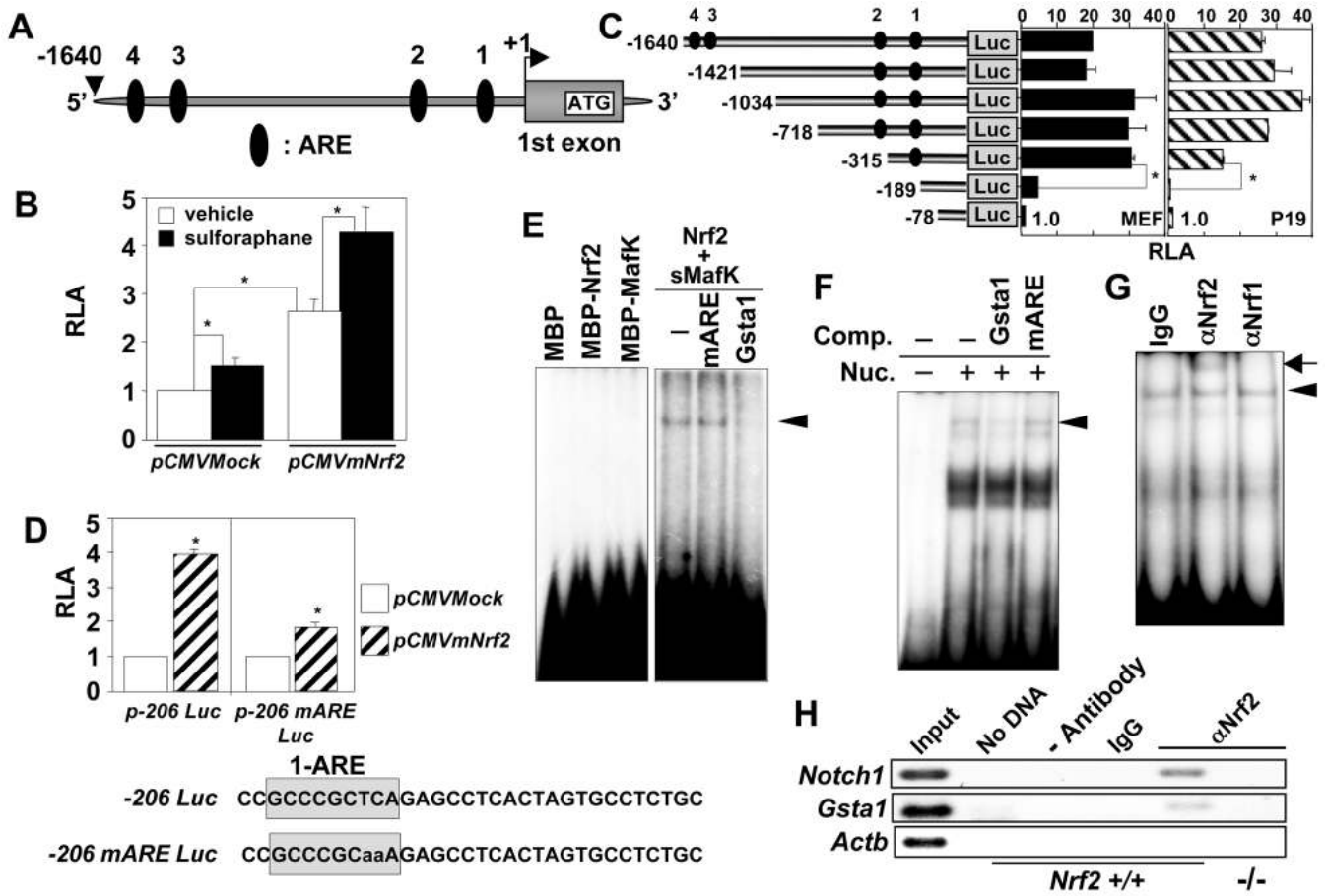


Fig. 2. Analysis of the proximal promoter of murine *Notch1* in MEFs

A ~2-kb portion of the promoter of *Notch1* was isolated from murine liver and ligated into a luciferase reporter vector (-1640 *Notch1*-Luc) to monitor its activity. A. Distribution of putative ARE motifs. B. Effect of the presence of Nrf2 and sulforaphane (2.5 μ M) treatment on -1640 *Notch1*-Luc reporter gene activity in MEFs. Values are mean \pm S.E. (n=3). * P < 0.05. Data are shown as the relative luciferase activity (RLA) compared to that in vector (*pCMV Mock*)-transfected cells in the absence of sulforaphane, which was set at a value of 1.0. C. Serial deletion assays of the -1640 *Notch1*-Luc reporter with relative luciferase activities in MEF (left) and P19 EC (right) cells shown. In both analyses, the activities from the -78 construct were set at a value of 1.0. Black ellipses show the presence of putative AREs. Values are mean \pm S.D. (n=3). Luciferase activities were normalized by measuring the *Renilla* luciferase activity from a cotransfected reporter vector. * P < 0.05. D. Effect of site-directed mutagenesis on the enhancer capacity of the 1-ARE motif in MEFs. Cells were either transfected with the -206 *Notch1*-Luc truncated promoter construct (p-206 Luc), which contained the 1-ARE, or with a form with point mutations in the 1-ARE (p-206 mARE Luc). RLA was based on the activity from each -206 Luc reporter construct when transfected with the vector *pCMV Mock*, which was set at a value of 1.0. Values are mean \pm S.D. * p < 0.05. E. Recombinant Nrf2 and MafK form a complex with *Notch1*-1-ARE, which can be competed away by the *Gsta1*-ARE but not mutant 1-ARE. Left panels show negative controls for the analysis. Right panels show EMSA in the presence of the ARE. F. Binding of nuclear factors from MEFs to the 1-ARE of *Notch1* can be competed away with the ARE of the mouse *Gsta1* promoter region (table S1), but not by mutant 1-ARE of *Notch1* (mARE). A 25-fold molar excess of each competitor was used. G. The binding complex can be supershifted with

an antibody to Nrf2, but not with an antibody to Nrf1 or with normal rabbit IgG. The arrowhead indicates the specific protein complex with the 1-ARE probe and the arrow indicates the supershifted band. H. ChIP assay using wild-type and *Nrf2*^{-/-} cells. No DNA and IgG reactions were the controls for PCR and immunoprecipitation steps, respectively. The 1-ARE in the *Notch1* gene regulatory region was detected only in the presence of wild-type cell nuclear extract and the antibody to Nrf2. The *Gsta1* promoter region, which has a functional ARE, served as a positive control.

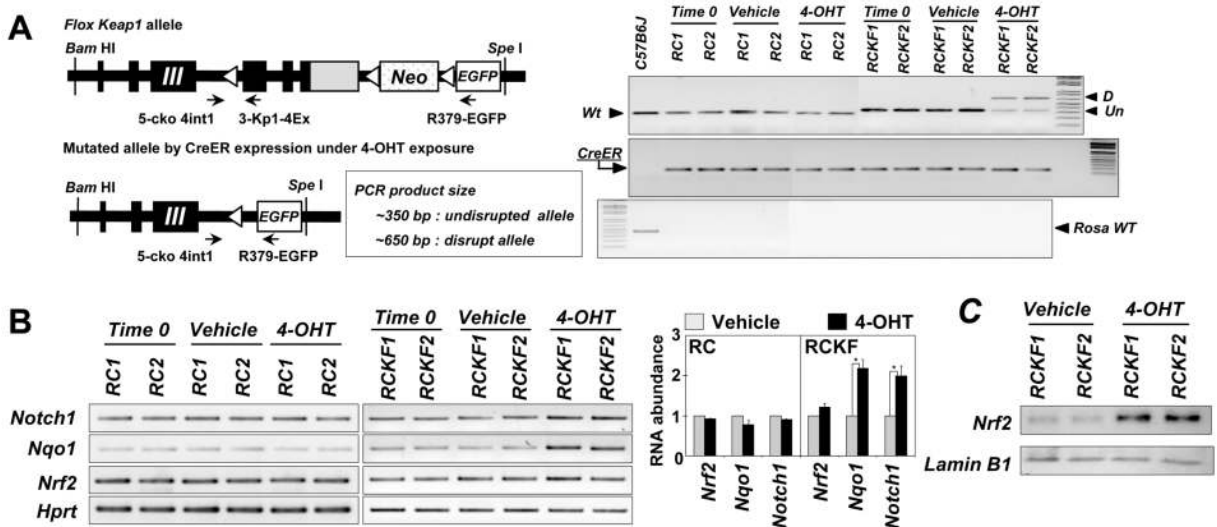


Fig. 3. The timing-specific induction of *Notch1* by *Nrf2* is shown with *Rosa^{CreER/CreER}::Keap1^{fllox/fllox}* (RCKF) MEF cells

A. Scheme of the genetic alleles present within the mouse constructs utilized: The mutant cell line carrying the floxed *Keap1* gene (top) and the expected disrupted allele (bottom).

Rosa^{CreER/CreER} MEF cells (RC1 and RC2), as well as RCKF1 and RCKF2 cells, were treated with 1 μ M 4-OHT for 3 days with repetitive treatments each 24 hours. D, disrupted gene; Un, undisrupted gene. B. Treatment with 4-OHT induces *Notch1* and *Nqo1* gene expression in RCKF MEF cells, as shown by RT-PCR. The magnitude of the expression of each gene was normalized by the expression of the housekeeping gene *Hprt* using the total RNA derived from both RC1 and RCKF1 MEF (right panel). Gene expression from vehicle treated samples in each cell was set at a value of 1.0. Values are mean \pm S.D. * $p < 0.01$ (n=3, one-way analysis of variance). C. Immunoblotting of *Nrf2* in the RCKF MEF cell extracts shows that *Nrf2* accumulates in cells following treatment with 4-OHT.

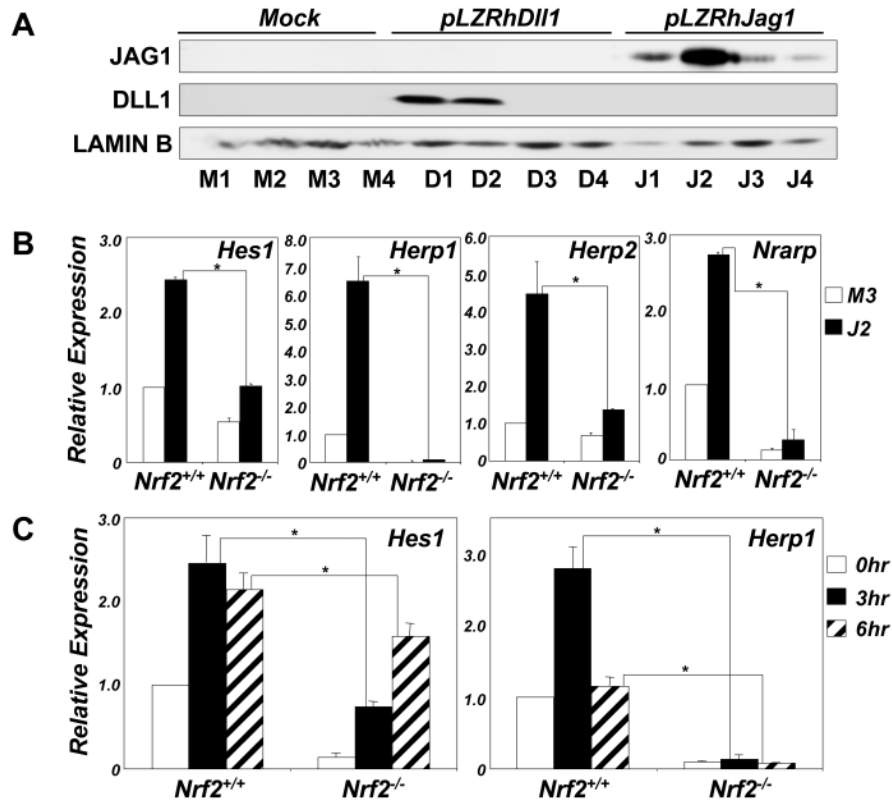


Fig. 4. In MEFs, Notch1 signaling is dependent upon *Nrf2* genotype

A. The abundance of Notch1 signaling ligands (DLL1 or JAG1) in independent lines of stably transfected HEK293 cells as shown by immunoblot analysis with JAG1 or DLL1 specific antibodies (sc-8303, sc-9102). Probing the blots with a Lamin B1 antibody (sc-6216) served as the loading control. M1-4, mock; D1-4, DLL1; J1-4, JAG1. B. Effect of *Nrf2* genotype on Notch1 signaling in MEFs co-cultured with JAG1-expressing HEK293 (J2) cells. C. Time course showing Notch1 signaling in MEF cells co-cultured with DLL1 expressing HEK293 (D2) cells. Gene expression in B and C was examined by real time reverse transcriptase PCR. *18S* ribosomal RNA expression was used for normalization. The expression for each gene in *Nrf2*^{+/+} MEF was set at a value of 1.0. Values are mean ± S.D. (n=3). *P< 0.05, one-way analysis of variance.

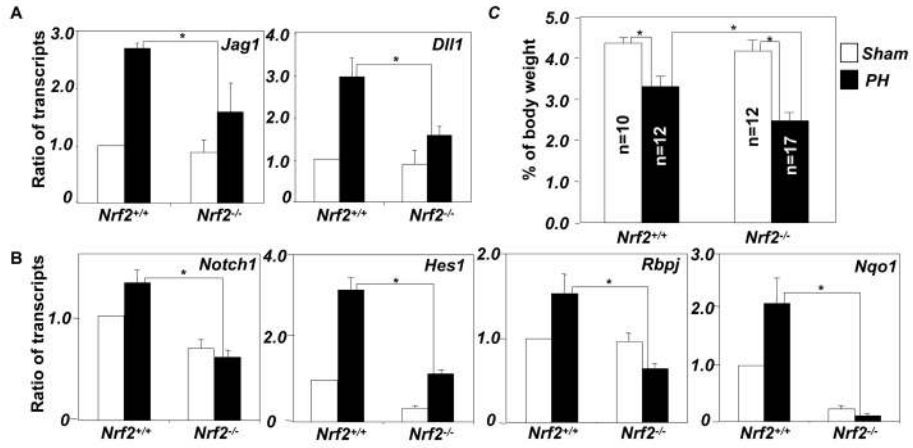


Fig. 5. Reduced basal Notch1 signaling in *Nrf2*-null mice delays liver regeneration

A. *Jag1* and *Dll1* expression in whole liver was analyzed by real-time reverse transcriptase PCR as ligands of Notch1 signaling 3 hr after 2/3 partial hepatectomy. *Hprt* expression was used for normalization. B. *Hes1* expression was monitored by real-time reverse transcriptase PCR as an index of Notch1 signaling 6 hr after 2/3 partial hepatectomy. *Albumin* expression was used for normalization. The ratio of hepatic gene of interest to albumin gene expression in sham-operated *Nrf2*^{+/+} mice was set at a value of 1.0. Values are mean \pm S.D., n = 3, * p < 0.05, one-way analysis of variance. C. Relative liver weights from *Nrf2*^{-/-} and wild-type mice (age and total body weight-matched) 3 days after 2/3 partial hepatectomy (PH). Values are mean \pm S.D. * p < 0.01, one-way analysis of variance. White boxes in A, B and C represent sham-operated animals; black boxes are partial hepatectomy animals.

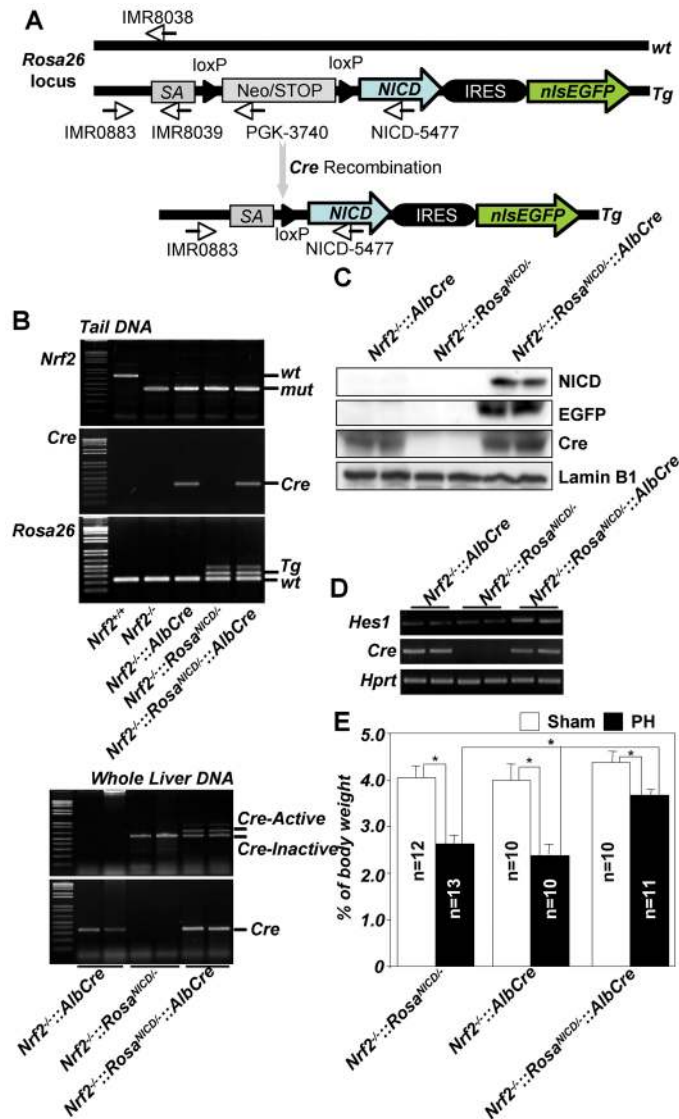


Fig. 6. NICD restores liver regeneration in *Nrf2*-null mice

A. Scheme for hepatocyte-specific NICD expression. Arrows show primers used for genotyping. Sequences are described in table S2. B. Demonstration of homologous recombination only in genomic DNA isolated from the livers of *Nrf2*^{-/-}::*Rosa*^{NICD/-}::*AlbCre* mice. Wt, Tg, mut and Cre stand for wild-type locus, transgenic *rosa 26* locus, *Nrf2* disrupted allele and *AlbCre* recombinase insertion allele. C. Immunoblots of NICD and EGFP demonstrating that the proteins were present only in the liver of *Nrf2*^{-/-}::*Rosa*^{NICD/-}::*AlbCre* mice. Lamin B1 served as the control for protein loading and was detected with an antibody. D. Hepatic expression of *Hes1* in *Nrf2*^{-/-}::*Rosa*^{NICD/-}, *Nrf2*^{-/-}::*AlbCre*, and *Nrf2*^{-/-}::*Rosa*^{NICD/-}::*AlbCre* mice. The ratios of hepatic *Hes1* expression are 0.58±0.13(SD), 4.31±0.72(SD) in *Nrf2*^{-/-}::*Rosa*^{NICD/-} and *Nrf2*^{-/-}::*Rosa*^{NICD/-}::*AlbCre*, respectively. *Hes1* expression in *Nrf2*^{-/-}::*AlbCre* was set at a value of 1.0. n=3, p<0.01, one-way analysis of variance. E. Regenerative recovery of liver mass in *Nrf2*^{-/-}::*Rosa*^{NICD/-}, *Nrf2*^{-/-}::*AlbCre* and *Nrf2*^{-/-}::*Rosa*^{NICD/-}::*AlbCre* mice. Values are mean ± S.D., * p < 0.01, one-way analysis of variance. White box, sham-operated animals; black boxes, partial hepatectomy animals.